Exploring the wavefront of hard X-ray laser radiation

S. Rutishauser, L. Samoylova, J. Krzywinski, O. Bunk, J. Grünert, H. Sinn, M. Cammarata, D. M. Fritz, and C. David

June 8, 2012

Supplementary figures

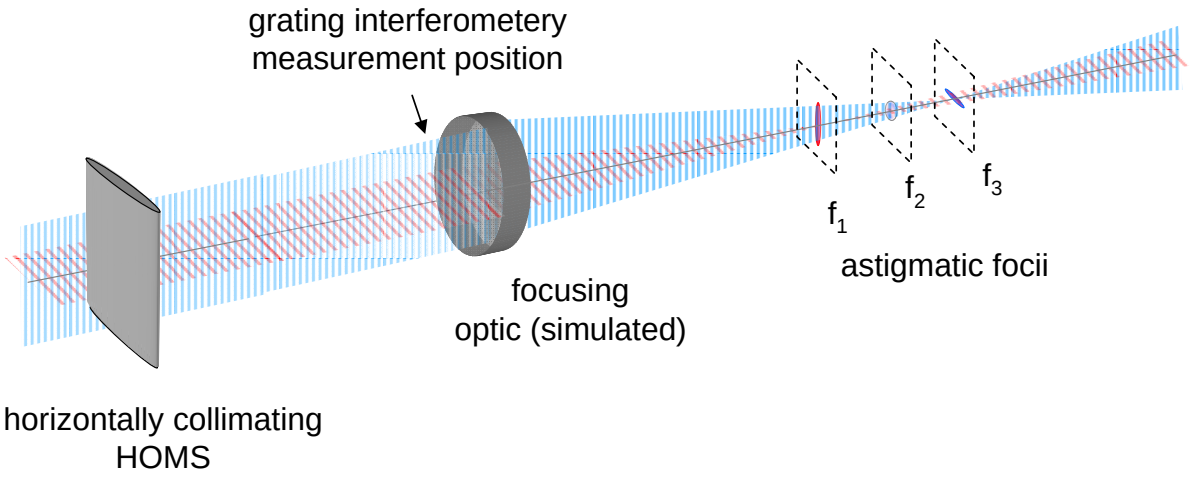

Supplementary Figure S1: **Setup sketch.** The spherical wavefront emitted by the source is horizontally collimated by the HOMS mirrors, and observed by the grating interferometer downstream. After propagation through a simulated ideal focusing optic, the wavefront is focused in horizontal direction (f_1) and slightly further downstream in vertical direction (f_3).

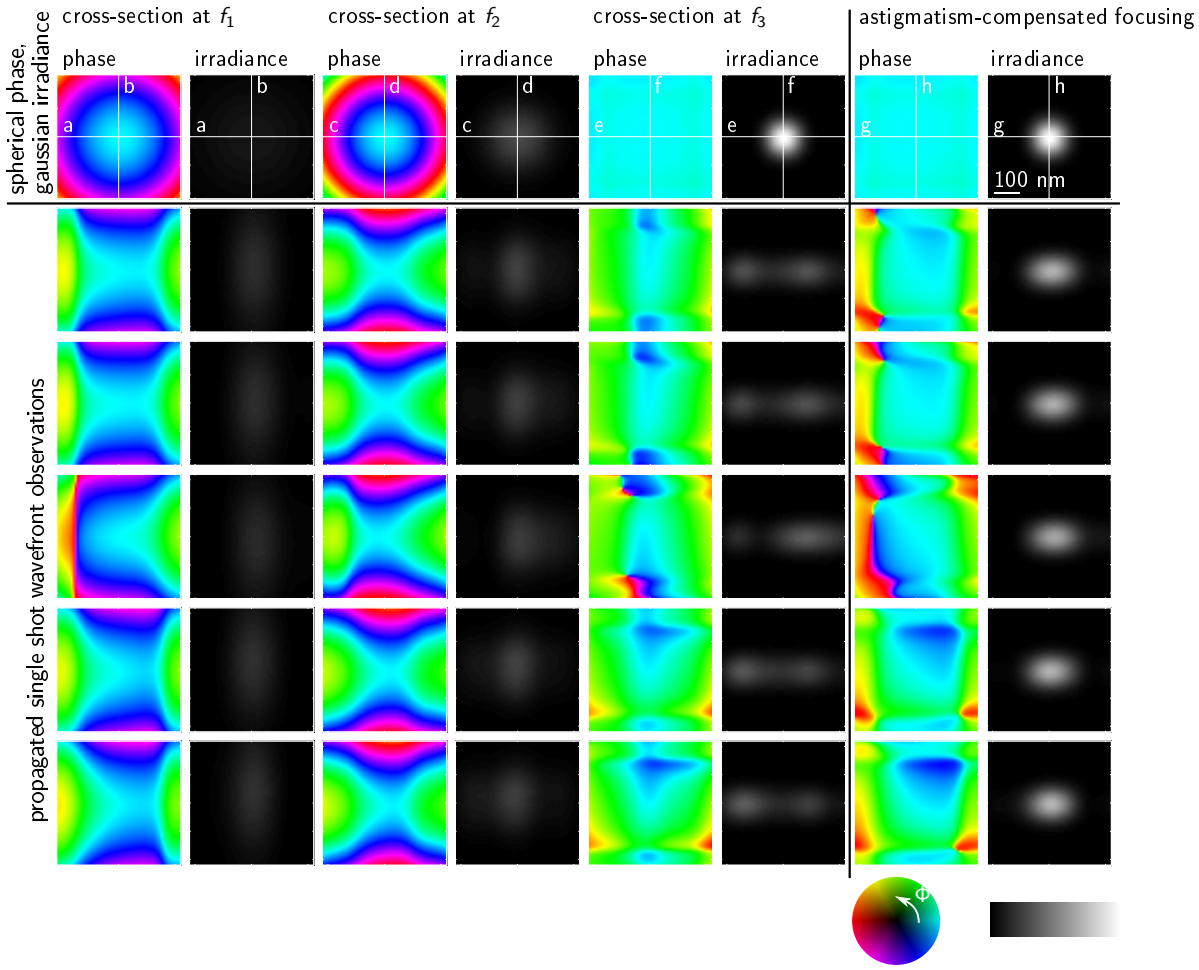

Supplementary Figure S2: Through-focus cuts. Phase and irradiance at positions f_1, f_2 and f_3. The two last columns show the focus of an optic that compensates for the astigmatism. The phase is encoded as hue in HSV color space. The irradiance has been normalized for all shots, to compensate for intensity fluctuations of the machine and only show the effects of wavefront distortions. The first line shows the profiles for an ideal Gaussian irradiance, the remaining profiles show the same five single shots as in Fig. 3.

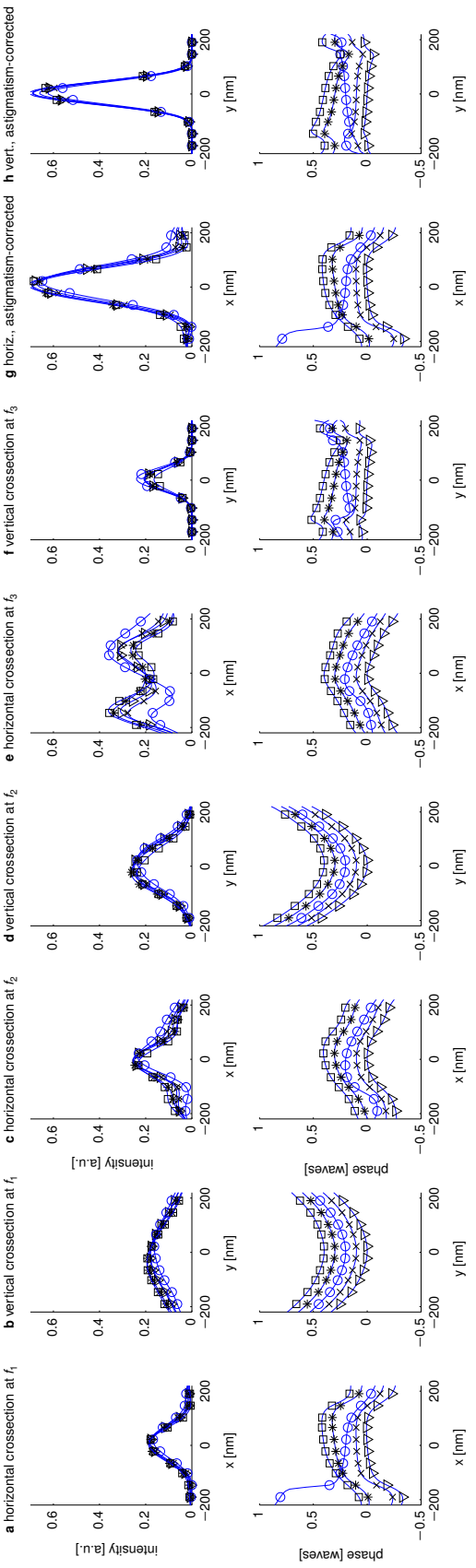

Supplementary Figure S3: Through-focus line plots. Irradiance and phase along the lines sketched in Supplementary Figure S2. The plotted five single shots are the same as in Fig. 3. The irradiance profiles are normalized to the maximum irradiance of an ideal spherical wavefront with Gaussian intensity distribution (profile not shown here). The wavefront phases of the single shots have been offset by 0.1 waves. (a - f) show the different astigmatic focii f_1 to f_3 (Supplementary Figure S1). (g - h) show the irradiance and phase profiles through the focus created by an optic that compensates for the differing horizontal and vertical wavefront curvature radii.

Supplementary methods

Simulated focal spot downstream of an ideal focusing optic

To demonstrate the consequences of wavefront distortions and shot to shot fluctuations, we have Fresnel-propagated the single-shot measured wavefront as shown in Fig. 3(a) through an ideal focusing optic with a focal length of 0.5 m. This represents is a typical focal length for nanofocusing at LCLS. A microfocusing optic with longer focal length produces wavefronts with very similar properties, but with a correspondingly larger focal spot, larger depth of focus and increased distance between the two astigmatic focii.

Supplementary Figure S1 shows a sketch of the interferometer, the simulated focusing optic and the resulting focii. Due to the collimating effect of the hard X-ray offset mirrors, the beam is horizontally focused at one position (f_1), and vertically focused at a position 0.5 mm further downstream (f_3). The center between the two line focii is at f_2, providing the smallest symmetric focal spot. Supplementary Figures S2 and S3 show transverse cross-sections and line plots through the beam at the horizontal focus f_1, the vertical focus f_3 and the symmetric focus f_2.

The power of all shots in the Supplementary Figures S2 and S3 has been normalised, that is, the integral over each of the irradiance cross-section plots in the Supplementary Figure S2 is the same. The apparent irradiance differences are therefore not due to shot to shot fluctuations of the power emitted by LCLS, but rather due to wavefront aberrations leading to imperfect focusing.

The spherical component of the HOMS distortions causes astigmatism, which shows up as a spherical phase component in the cross-sections in the Supplementary Figure S3(b - e) and as symmetric color change along the corresponding profiles in Supplementary Figure S2. These spherical distortions are stable over time and independent of the irradiance profile. As a consequence of the astigmatism, the maximal attained power density is reduced by a factor of three with respect to an aberration-free illumination, as the beam is never simultaneously focused in both vertical and horizontal direction.

The non-spherical components of the wavefront distortions (higher order aberrations) produced by the HOMS propagate into significant irradiance and phase variations of the beam profile, which strongly depend on the irradiance distribution of the individual shots.

It is interesting to see that the phase the third shot (blue circle markers in Fig. 3 and Supplementary Figure 3), which represents about 10% of observed shots we observed, has opposite slope in the horizontal and vertical focus, when compared to the other shots [Supplementary Figure S3(a) and (f)]. It also differs from the other shots in the intermediate focus [Supplementary Figure S3(c)].

The astigmatism can only be compensated for by using a focusing system, where the horizontal and vertical focal length or the working distance can be adjusted independently. This is the case for Kirkpatrick-Baez (KB) focusing mirror systems, for Fresnel zone plates which could be fabricated in elliptical shape, or for combinations of one-dimensional refractive lenses.

Simulating an optic that perfectly compensates the astigmatism introduced by the HOMS, the intensity and phase distributions shown in the last columns of Supplementary Figures S2

and S3 are obtained. As a consequence, the power density in the focus is increased to about 70% of an ideal non-aberrated focus, and the illumination profile becomes homogeneous.

Having subtracted the effect of the spherical distortion, all remaining distortions are due to higher order aberrations. One of their consequences is that the focal spot is larger in horizontal direction than in the vertical, leading to a loss in power density. While the phase in the focus is quite flat, the shot with blue circle markers again shows an opposite phase slope in the focus. The wavefront slope change with respect to the other shots is about 0.2 waves over a focal spot size of 200 nm, which corresponds to a wavefront angle of 140 μrad. This is about 1/4 of the aperture angle of the focusing optic. The impact of such a shot to shot phase fluctuation depends on the specific experiment.

These effects are observed even with an ideal focusing optic and despite of the very high figuring quality of the offset mirror substrates. This underlines the usefulness of online wavefront monitoring of an out-coupled fraction of the beam or the non-diffracted radiation downstream of a sample in an “intelligent beamstop”, which could be used to observe the properties of each shot and compensate for such effects.